

Multivariate Links Between the Developmental Timing of Adversity Exposure and White Matter Tract Connectivity in Adulthood

Lucinda M. Sisk, Taylor J. Keding, Emily M. Cohodes, Sarah McCauley, Jasmyne C. Pierre, Paola Odriozola, Sahana Kribakaran, Jason T. Haberman, Sadie J. Zacharek, Hopewell R. Hodges, Camila Caballero, Gillian Gold, Audrey Y. Huang, Ashley Talton, and Dylan G. Gee

ABSTRACT

BACKGROUND: Early-life adversity is pervasive worldwide and represents a potent risk factor for increased mental health burden across the lifespan. However, there is substantial individual heterogeneity in associations between adversity exposure, neurobiological changes, and mental health problems. Accounting for key features of adversity such as the developmental timing of exposure may clarify associations between adversity, neurodevelopment, and mental health.

METHODS: In the current study, we leveraged sparse canonical correlation analysis to characterize modes of covariation between adversity exposure across development and the connectivity of white matter tracts throughout the brain in a sample of 107 adults.

RESULTS: We found that adversity exposure during preschool age and middle childhood (ages 4–5 and 8 years in particular) were consistently linked across diffusion metrics with alterations in white matter tract connectivity. Whereas tracts supporting sensorimotor functions showed higher connectivity with higher preschool-age and middle childhood adversity exposure, tracts supporting cortico-cortical communication showed lower connectivity. Furthermore, latent patterns of tract connectivity associated with adversity experienced across preschool age and middle childhood (ages 3–8) were associated with posttraumatic stress symptoms in adulthood.

CONCLUSIONS: Our findings underscore that adversity exposure may differentially affect white matter in a function- and developmental timing-specific manner and suggest that adversity experienced from ages 3 to 8 years may shape the development of white matter tracts across the brain in ways that are relevant for mental health in adulthood.

<https://doi.org/10.1016/j.bpsc.2025.02.003>

Up to 60% of youths are exposed to adverse childhood experiences (1). Childhood adversity is a potent predictor of mental health problems later in life (2); however, there is substantial variability in the onset and severity of psychiatric disorders following adversity exposure at the individual level. Specific aspects of adversity exposure such as the type, timing, and subjective perception of adverse events may contribute to this heterogeneity in outcomes (3–6). Given ongoing maturation of neural systems that support cognition, emotion, and sensorimotor functioning throughout childhood and adolescence, the developmental timing of exposure may modulate the impacts of adversity on neurodevelopment and later mental health (7,8). Identifying specific developmental stages during which adversity exposure disproportionately shapes the developing brain in ways that elevate psychiatric risk is an important step toward delineating the neural mechanisms that link adversity exposure and mental health burden.

Clarifying associations between adverse childhood experiences, neural structure, and mental health requires

consideration of neurodevelopment. The brain matures along a sensorimotor-association axis, such that cortical regions supporting sensorimotor functioning mature earlier in childhood, while higher-order association and transmodal integration regions mature later in adolescence and early adulthood (9,10). Given that the brain develops in a modular, circuit-specific manner (11,12), the relative maturational state of neural circuitry at the time of adversity exposure may inform how the exposure affects subsequent neurodevelopment and behavior (7,8,13–17). Typical neurodevelopment includes windows of heightened plasticity, during which circuits display increased sensitivity to environmental input pertinent to their function (18,19). During these windows, circuits may be particularly vulnerable to function-relevant adverse events (20–22), resulting in changes disproportionate to the same event experienced during a different developmental period (14). In this manner, circuit-specific, experience-dependent neuroplasticity may underlie the differential effects of adverse experiences on neural circuitry and mental health depending

on the timing of exposure, contributing to cascading individual differences across development.

Cross-species evidence demonstrates timing-specific associations between adversity exposure and neurodevelopment (23–26). While such work has largely focused on stress-sensitive regions such as the hippocampus, amygdala, and prefrontal cortex (8,27,28), research has also examined white matter connectivity between these and other regions. For example, exposure to adversity during the preadolescent period has been associated with reduced volume of the corpus callosum, the primary white matter tract that supports inter-hemispheric cortical communication (29,30), while severe neglect during early childhood has been associated with global, brainwide microstructural alterations (31,32). Adversity during early childhood has been associated with both lower connectivity of fiber populations involved in communication among association and limbic regions and higher connectivity of fiber populations involved in sensory processing (31–33). These findings suggest a negative association between adversity and white matter connectivity in tracts supporting higher-order processing and raise the possibility that the direction of associations between adversity exposure and tract connectivity may diverge depending on tract function and/or developmental stage. Research systematically examining associations between adversity exposure across development and white matter tract connectivity across the brain may yield relevant insights.

Due to the critical role of white matter tracts in relaying information within and between developing cortical regions, white matter tract connectivity is of particular interest when considering how the developmental timing of adversity relates to brain circuitry. Building on foundational research that identified critical periods for visual perception in nonhuman animals (19), our current understanding of developmental neuroplasticity suggests that multiple cellular mechanisms govern normative, circuit-specific increases and decreases in plasticity over the course of development (34,35). Among these, myelination, the process by which axons become enrobed in a fatty myelin sheath (36), can respond in an experience-dependent manner to refine neural pathways. More active axonal pathways are preferentially myelinated, while less active axonal pathways display decreased myelination (37,38). Thus, the responsiveness of myelination to experiential input suggests that it may contribute to both adaptive neurobiological changes and adversity-associated changes that potentiate psychiatric risk, particularly during adolescence (14,39). Probing how myelination is implicated in adversity-related alterations in the connectivity of large-scale white matter tracts—and whether this varies by timing of adversity—will facilitate greater understanding of neural responses in the face of challenging experiences (18,40).

In the current study, we leveraged a data-driven approach (sparse canonical correlation analysis [sCCA]) to examine covariation between adversity exposure during development and connectivity in 43 white matter tracts across the brain, as well as whether these patterns of covariation are associated with mental health symptoms. To identify patterns across metrics of tract connectivity that provide complementary insight into underlying mechanisms, we utilized 3 independent models to evaluate links between adversity and

generalized fractional anisotropy (GFA) (41), quantitative anisotropy (QA) (42), and radial diffusivity (RD) (43). Both GFA and QA are thought to index multiple cellular properties such as fiber orientation, density, and myelination, broadly referred to as tract connectivity. Whereas GFA indexes fiber connectivity at the voxel level, QA estimates these properties for the primary fiber orientation contained within the voxel, potentially yielding more accurate tract-level estimates (42). RD, also computed at the voxel level, measures the degree of water diffusion perpendicular to the primary diffusion direction and is sensitive to myelination, such that higher RD may indicate lower myelin content (44). We chose GFA and QA to facilitate interpretability given the wide usage of fractional anisotropy in studies that have examined adversity exposure and structural connectivity (45), and we selected RD as a proxy measure for myelination.

Informed by a rich literature on the neurodevelopmental effects of early childhood adversity (31), we hypothesized that greater exposure to adversity from the ages of 0 to 3 years would be linked to widespread decreases in tract connectivity as measured by GFA and QA, with the most pronounced negative associations being observed in the uncinate fasciculus and corpus callosum. Second, given evidence that adolescence may represent a period of heightened plasticity for association cortex neurodevelopment (10,46), we hypothesized that a measure related to myelin content (RD) in tracts that connect regions of association cortex (e.g., the superior longitudinal fasciculus, the inferior longitudinal fasciculus) would be negatively linked to adversity exposure during adolescence (ages 11–15). Finally, we predicted that the previously hypothesized variates (representing adversity during early childhood and connectivity of the uncinate fasciculus and corpus callosum) would both also be associated with symptomatology during adulthood (28,30,47–53).

METHODS

Participants

Participants were 107 adults between the ages of 18 and 30 years recruited from the broader New Haven, Connecticut, community. See [Supplemental Methods](#) for details on exclusion criteria. Study procedures were approved by the Yale University Institutional Review Board, and each participant provided informed consent in writing. Study participation consisted of 2 visits. During the first visit, participants completed the Dimensional Inventory of Stress and Trauma Across the Lifespan (DISTAL) (54) interview as well as questionnaires assessing mental health symptoms. During the second visit, participants completed a magnetic resonance imaging scan session with sequences including anatomical scans and a diffusion-weighted imaging scan.

Demographic Variables

Participants reported their age at scan session, sex assigned at birth, years of education, annual household income, and race and ethnicity. Additional demographic information can be found in [Table 1](#).

Adversity Timing and White Matter Tract Connectivity

Table 1. Sample Demographic Information (N = 107)

	Included in Symptom Analyses, n = 79	Not Included in Symptom Analyses, n = 28	Total, N = 107	<i>p</i> Value
Age at Scan, Years				.372
Mean (SD)	22.733 (3.081)	23.360 (3.449)	22.897 (3.177)	
Range	18.136–30.131	18.062–30.897	18.062–30.897	
Age at DISTAL, Years				.352
Mean (SD)	22.661 (3.078)	23.314 (3.427)	22.832 (3.169)	
Range	18.125–30.109	18.048–30.829	18.048–30.829	
Sex Assigned at Birth				.215
Female	49 (62.0%)	21 (75.0%)	70 (65.4%)	
Male	30 (38.0%)	7 (25.0%)	37 (34.6%)	
Gender Identity				.141
Cisgender female	49 (62.8%)	20 (71.4%)	69 (65.1%)	
Cisgender male	29 (37.2%)	7 (25.0%)	36 (34.0%)	
Transgender female	0 (0.0%)	0 (0.0%)	0 (0.0%)	
Transgender male	0 (0.0%)	1 (3.6%)	1 (0.9%)	
Missing data	1	0	1	
Education, Years				.643
High school	11 (13.9%)	3 (10.7%)	14 (13.1%)	
College	52 (65.8%)	17 (60.7%)	69 (64.5%)	
Graduate school	16 (20.3%)	8 (28.6%)	24 (22.4%)	
Combined Annual Income				.775
<\$5000	4 (5.1%)	1 (4.8%)	5 (5.0%)	
\$5000–\$11,999	2 (2.5%)	2 (9.5%)	4 (4.0%)	
\$12,000–\$14,999	3 (3.8%)	2 (9.5%)	5 (5.0%)	
\$15,000–\$24,999	8 (10.1%)	1 (4.8%)	9 (9.0%)	
\$25,000–\$34,999	6 (7.6%)	1 (4.8%)	7 (7.0%)	
\$35,000–\$49,999	7 (8.9%)	1 (4.8%)	8 (8.0%)	
\$50,000–\$74,999	19 (24.1%)	5 (23.8%)	24 (24.0%)	
\$75,000–\$99,999	4 (5.1%)	2 (9.5%)	6 (6.0%)	
\$100,000+	26 (32.9%)	6 (28.6%)	32 (32.0%)	
Missing data	0	7	7	
Race and Ethnicity				.913
Asian	15 (19.0%)	6 (21.4%)	21 (19.6%)	
Black or African American	9 (11.4%)	4 (14.3%)	13 (12.1%)	
Hispanic or Latinx	7 (8.9%)	4 (14.3%)	11 (10.3%)	
Multiracial	6 (7.6%)	2 (7.1%)	8 (7.5%)	
Non-Hispanic White	41 (51.9%)	12 (42.9%)	53 (49.5%)	
Missing data	1 (1.3%)	0 (0.0%)	1 (0.9%)	
RI PTSD Symptoms				.058
Mean (SD)	19.354 (16.447)	6.333 (5.955)	18.435 (16.265)	
Range	0.0–69.0	0.0–15.0	0.0–69.0	
Missing data	0	22	22	
TSC-40 Symptoms				.825
Mean (SD)	16.756 (12.731)	16.053 (10.911)	16.619 (12.345)	
Range	0.0–63.0	0.0–37.0	0.0–63.0	
Missing data	1	9	10	
ASR Total Problems T Score				.128
Mean (SD)	44.987 (9.287)	41.821 (9.657)	44.159 (9.443)	
Range	28.0–71.0	27.0–64.0	27.0–71.0	

Table 1. Continued

	Included in Symptom Analyses, <i>n</i> = 79	Not Included in Symptom Analyses, <i>n</i> = 28	Total, <i>N</i> = 107	<i>p</i> Value
Site				.007
Brain Imaging Center	37 (46.8%)	5 (17.9%)	42 (39.3%)	
Magnetic Resonance Research Center	42 (53.2%)	23 (82.1%)	65 (60.7%)	

Values are presented as *n*, *n* (%), mean (SD), or range. Demographic information is shown for age at scan session, age at DISTAL interview, sex assigned at birth, gender identity, years of education, combined family income, race and ethnicity, posttraumatic stress disorder (PTSD) symptoms (RI), trauma-related symptoms (TSC-40), total problems T scores (ASR), and site of scan acquisition. Because some participants had missing data required for symptom analyses, we report group differences for the sample used for symptom analyses. χ^2 Tests were used to evaluate differences between groups for ordinal and categorical data, and *t* tests were used to evaluate differences for continuous data.

DISTAL, Dimensional Inventory of Stress and Trauma Across the Lifespan; RI, Reaction Index; TSC-40, Trauma Symptom Checklist-40.

Interview and Assessment of Adversity Exposure (Visit 1)

Participants completed the DISTAL interview, which is broadly based on the structure of the University of California at Los Angeles Posttraumatic Stress Disorder Reaction Index (UCLA PTSD RI) interview (55) and is designed to assess key dimensions of adverse exposures including age of exposure (54). Details can be found in the [Supplemental Methods](#). For each type of event that was reported in the screening portion of the interview, participants were asked to report on the cumulative list of ages at which they experienced the event (0–30, or 0 through the participant's current age if <30). Cleaned data were then summed to derive a total count of adverse events at each year of age from ages 0 to 30 years (or 0 through the participant's current age) (Table S1 and Figure S1).

Mental Health Symptoms (Visit 1)

Following administration of the DISTAL interview (54), PTSD symptoms were assessed using the symptom scale from the UCLA PTSD RI (55). See [Supplemental Methods](#) for additional details. General trauma-related symptoms—not specific to a focal event—were assessed with the Trauma Symptoms Checklist (TSC-40) (56). Total mental health symptom T scores were derived from the Adult Self-Report Scale (ASR) (57).

Scanning Session (Visit 2)

Participants were scanned on 3T Siemens Magnetom Prisma scanners (Siemens) using a 32-channel head coil. Additional details, including scan parameters, can be found in [Supplemental Methods](#).

FreeSurfer Preprocessing

T1-weighted images were submitted to FreeSurfer 6.0.0 and processed using the *recon_all* pipeline (58). The resulting estimated total intracranial volume values for each participant were regressed from white matter tract data in subsequent modeling to address variability in white matter tract connectivity related to overall head size. Descriptive statistics for estimated total intracranial volume are presented in Table S2.

QSIprep Preprocessing and Reconstruction

Preprocessing was performed using QSIprep 0.14.3 (59). Preprocessing details can be found in [Supplemental Methods](#). Anatomical data were corrected for intensity nonuniformity,

skull stripped, and spatially normalized using ANTS 2.3.1 (60). Brain tissue segmentation was performed using FSL's FAST (61). Diffusion data were denoised, corrected for ringing and B1 field inhomogeneity, and intensity-matched across B0 images using tools from MRtrix (62,63). Next, FSL's eddy tool was used for head motion and eddy current correction as well as outlier replacement (64). Finally, data were resampled to 1-mm isotropic voxels in anterior commissure–posterior commissure (AC-PC) space. Descriptive statistics for motion metrics produced by QSIprep are presented in Table S2. Diffusion data were reconstructed using QSIprep workflows leveraging DSISudio and MRtrix, and tractography was performed using TractSeg (65). For further details regarding diffusion data reconstruction and tractography, see [Supplemental Methods](#).

Experimental Design and Statistical Analysis

Data Preparation. Analyses were conducted in Python (66), and tables were created in R (67). Covariates were regressed from white matter tract data and adversity exposure data separately. We regressed age at scan session, estimated total intracranial volume, mean framewise displacement during the diffusion scan, a binary indicator of scan site, and mean connectivity of the metric (GFA, QA, or RD) from the white matter tract data and age at DISTAL interview session, sex assigned at birth, and the total number of adversity exposures during adulthood from the adversity exposure data. For additional details, see [Supplemental Methods](#).

Model Fitting. Three separate sCCA models were fitted using the package *cca-zoo* (68). We use the term *mode* to refer to pairs of correlated variates identified by the sCCA model. The term *variate* refers to a latent variable representing a linear combination of key variables from one of the datasets submitted to sCCA that is correlated with a paired latent variable representing a linear combination of key variables from the other dataset submitted to sCCA. Greater mathematical detail and discussion of these terms can be found in previous publications (69,70). Here, we fitted models examining links between the developmental timing of adversity exposure and GFA, QA, and RD, respectively, across white matter tracts (Figure 1A). We reasoned that because these metrics measure overlapping properties of underlying white matter but may be differentially sensitive to cellular properties that vary as a function of development, identifying measure-specific links

Adversity Timing and White Matter Tract Connectivity

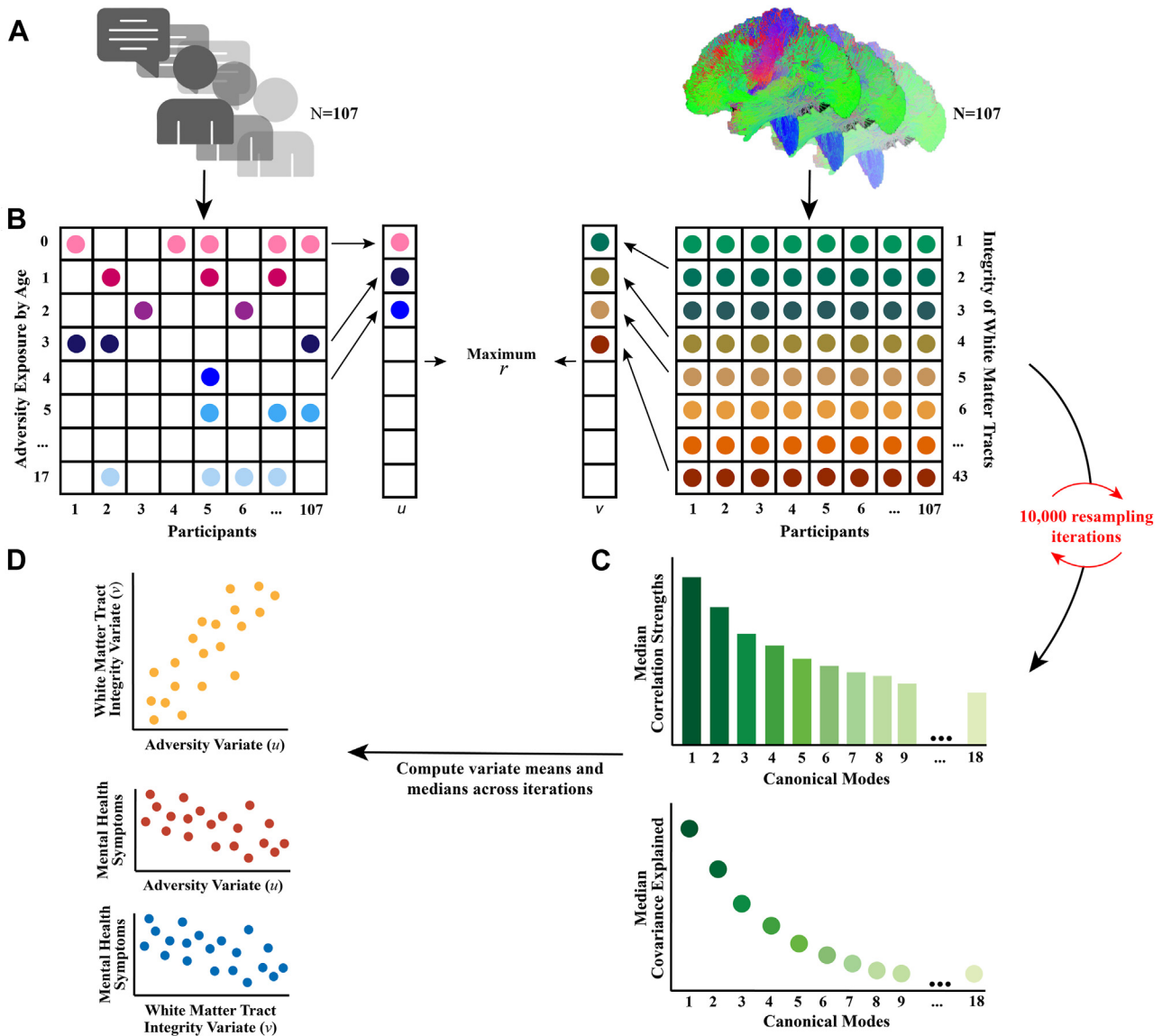


Figure 1. Schematic of approach. **(A)** Dimensional adversity exposure data from the Dimensional Inventory of Stress and Trauma Across the Lifespan (left) and white matter tract connectivity measures from 43 tracts (right) were submitted to sparse canonical correlation analysis (sCCA). **(B)** Eighteen sCCA modes were fitted per sCCA model, and this process was repeated 10,000 times with resampling. For each iteration, a shuffled (null) model was also fitted. **(C)** For each iteration, correlation strengths for each mode and covariance explained for each mode were retained, as were variable loadings for each variate of each mode. **(D)** sCCA variates maximize correlation strengths. Following sCCA modeling, associations between transformed participant-level variate data and mental health symptoms were tested.

with adversity data would yield more interpretable insights into how adversity timing is associated with white matter tract properties. To identify the most robust patterns of association, we fitted both an unshuffled model and a shuffled (null) model across 10,000 resampling iterations (Figure 1B). For each iteration, we fitted an sCCA model with 18 modes and computed covariance explained and correlation strengths for each mode (Figure 1C). To evaluate model significance, we fully shuffled the adversity data and computed covariance explained and correlation strengths from the resulting null

model. To evaluate the significance of the unshuffled models relative to the shuffled models, we used permutation testing (71). We opted to use the median as a representative metric because the correlation values did not follow a Gaussian distribution. Then, we corrected for multiple comparisons across modes that explained more than 10% of the overall covariance using false discovery rate (FDR) correction (72).

Associations With Symptoms. To test whether the identified variates were associated with mental health symptoms,

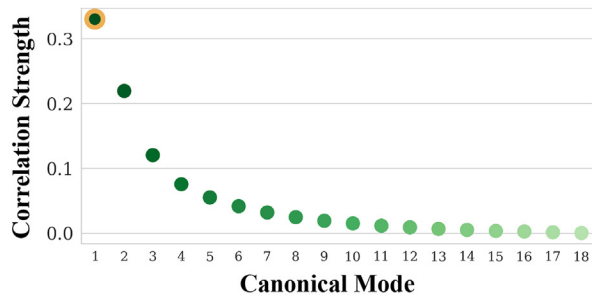
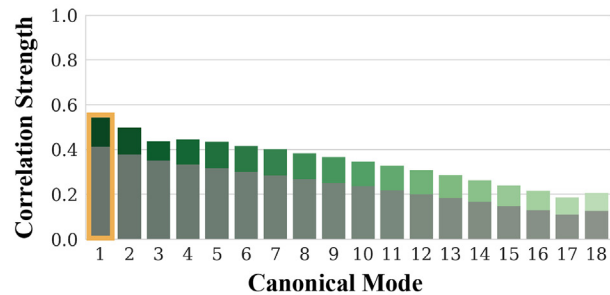
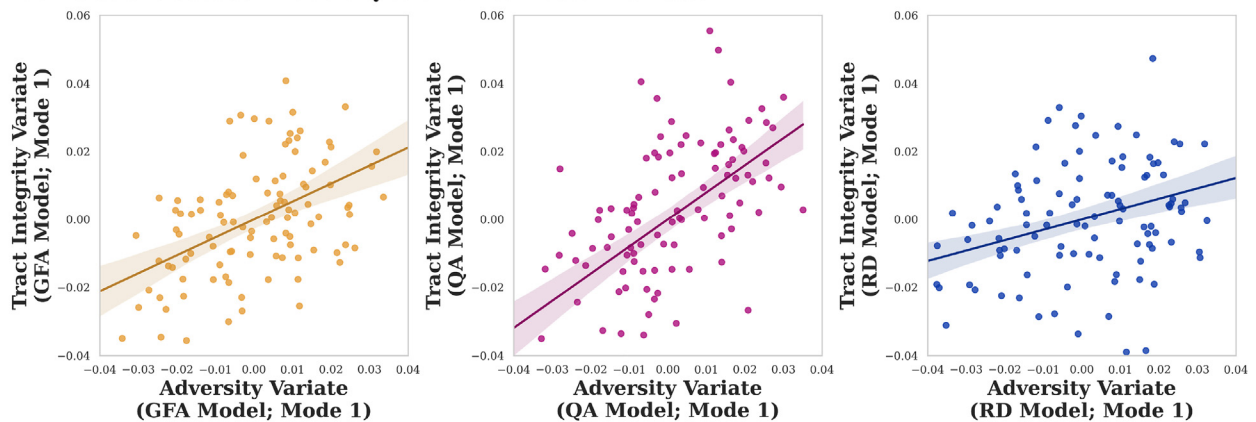
A Covariance Explained by Canonical Mode (GFA Model)**B Correlation Strength by Canonical Mode (GFA Model)****C Correlations between Adversity and White Matter Variates**

Figure 2. Model covariance explained and correlation strengths exemplified in the generalized fractional anisotropy (GFA) model. **(A)** Median covariance explained by each canonical mode over 10,000 iterations of resampling. **(B)** Median correlation strengths between the variates of the 18 canonical modes over 10,000 iterations of resampling. The median correlation strengths between variates of the shuffled (null) model over 10,000 iterations of resampling are overlaid in gray on the median correlation strengths between variates of the unshuffled model (green). **(C)** Associations between the adversity and white matter variates of each of the 3 models (GFA, quantitative anisotropy [QA], radial diffusivity [RD]) averaged across 10,000 resampling iterations.

for each model fit across 10,000 resampling iterations, we subsequently transformed the input data using the fitted model, which resulted in participant-level values for adversity and white matter variates across all fitted modes. Next, we computed mean participant-level values for the adversity and white matter variates of the first mode across all iterations. Consistent with our previous decision to focus solely on the first mode, here we examined only the transformed data representing white matter and adversity variates of the first mode in each of the GFA, QA, and RD models. We tested whether symptoms (posttraumatic stress symptoms, general trauma-related symptoms, and total symptoms T scores) were associated with sCCA model variates by fitting an ordinary least squares (OLS) model per each symptom measure for the adversity variates of the 3 models and a separate OLS model for the white matter variates of 3 models (Figure 1D). We used FDR correction to account for multiple comparisons across the 3 symptom measures. We opted to test white matter and adversity variates in separate models because by design sCCA identifies adversity and white matter variates that are highly correlated, and including them in the same model could destabilize effect estimations. In all models, we used the variance inflation factor (VIF) to confirm that sCCA-derived

variates were not problematically collinear (all VIFs <2) and the Jarque-Bera test to confirm that model residuals followed a normal distribution. For outcomes, see [Supplemental Methods](#). Given broad evidence that socioeconomic status is a proxy for experiences that may shape brain development (73,74) and may covary with measures of adversity such that children who grow up in households with lower socioeconomic status are at heightened risk of experiencing adversity (13,75), we included combined family income and years of education as covariates.

Sensitivity Analyses. We conducted sensitivity analyses for variables that loaded onto variates that were associated with symptoms. Further details can be found in the [Supplemental Methods](#) and [Supplemental Results](#).

RESULTS**sCCA Model Fitting**

For each of the 3 white matter metrics of interest (GFA, QA, and RD), we fit separate sCCA models with resampling across 10,000 iterations, with the number of modes set to the number

Adversity Timing and White Matter Tract Connectivity

Table 2. Loading Significance for Variables on the Adversity Variate of Mode 1 Across Models

Variable	GFA Model		QA Model		RD Model	
	Wilcoxon Stat	p_{FDR}	Wilcoxon Stat	p_{FDR}	Wilcoxon Stat	p_{FDR}
Exposure at Age 0	11,282,221	<.001	17,631,745	<.001	21,052,192	<.001
Exposure at Age 1	11,163,381	<.001	17,482,028	<.001	21,105,858	<.001
Exposure at Age 2	15,931,135	<.001	17,541,155	<.001	23,579,364	<.001
Exposure at Age 3	24,147,121	.003	20,691,305	<.001	23,851,108	<.001
Exposure at Age 4	21,375,514	<.001	17,904,410	<.001	23,835,512	<.001
Exposure at Age 5	22,355,166	<.001	19,324,401	<.001	23,710,829	<.001
Exposure at Age 6	22,133,489	<.001	20,301,052	<.001	24,869,900	.684
Exposure at Age 7	22,151,724	<.001	21,812,695	<.001	24,902,450	.729
Exposure at Age 8	23,082,528	<.001	23,118,645	<.001	24,800,180	.544
Exposure at Age 9	24,870,451	.647	24,997,300	.986	24,240,741	.012
Exposure at Age 10	23,344,031	<.001	24,391,621	.041	23,983,219	.001
Exposure at Age 11	24,061,252	.001	23,633,333	<.001	24,379,143	.04
Exposure at Age 12	24,466,502	.067	24,695,981	.324	22,924,521	<.001
Exposure at Age 13	23,509,833	<.001	24,778,888	.464	23,098,886	<.001
Exposure at Age 14	23,405,282	<.001	23,497,790	<.001	22,977,940	<.001
Exposure at Age 15	20,889,288	<.001	22,009,069	<.001	24,537,074	.128
Exposure at Age 16	24,062,004	.001	24,205,767	.007	22,922,860	<.001
Exposure at Age 17	22,968,648	<.001	22,197,669	<.001	23,795,399	<.001

FDR, false discovery rate; GFA, generalized fractional anisotropy; QA, quantitative anisotropy; RD, radial diffusivity.

of adversity measures submitted to the model (18 modes). We aimed to identify 1) whether mode correlation strength differed significantly between the unshuffled (fitted) and shuffled (null) models, and 2) which modes explained the greatest proportion of total covariance. Across all models, the first mode explained the greatest amount of covariance (Figure 2A) and had the strongest correlation between mode variates (white matter and adversity variates) (Figure 2B). In addition, the first mode (Figure 2B) had a greater correlation strength than the first mode of the null model [all $ps < .05$ after FDR correction (72)]. Thus, we opted to examine only the first mode for each of the GFA, QA, and RD models to further avoid the potential for inflated significance of subsequent modes as a result of permutation testing (76). The correlated variates comprising the first modes for each of the 3 models (GFA, QA, and RD; averaged across 10,000 iterations) are plotted (Figure 2C).

GFA Model. Next, we tested whether variables that loaded onto model variates (i.e., adversity and white matter contributors to a given mode) in unshuffled models differed significantly from the variables that loaded onto model variates in shuffled models using Wilcoxon tests (77). For the adversity variate of the GFA model, all adversity exposure variables differed significantly between the unshuffled model loadings and the shuffled model loadings with the exception of exposure to adversity at ages 9 and 12 (Wilcoxon tests, $p_{FDR} < .05$) (Table 2). All white matter tract loadings differed significantly from the shuffled model except for the right optic radiation tract (Wilcoxon tests, $p_{FDR} < .05$) (Table 3). To identify which variables were most strongly represented in the first variate, we examined the median loading values for variables that loaded onto the adversity and white matter variates across 10,000 bootstrapped model fits, excluding nonsignificant variables.

Because variables could load both positively and negatively, we used the absolute value of the median loading as an index of a given variable's importance and examined the top 25% most important variables. The top loadings for the adversity variate were adversity experienced during ages 1 and 0 years followed by adversity experienced during ages 4, 8, and 5 years, respectively. All adversity variables loaded negatively. For the white matter variate, loadings representing the connectivity of the bilateral corticospinal tracts, parietal occipital-pontine tracts, and frontopontine tracts were strongest, followed by the right superior longitudinal fasciculus III tract, corpus callosum splenium, bilateral superior thalamic radiation tracts, and the corpus callosum isthmus. The superior longitudinal fasciculus tract and corpus callosum isthmus loaded positively, while the corticospinal tracts and corticopontine tracts loaded negatively (Figure 3A).

QA Model. For the QA model, all adversity exposure variables differed significantly between the unshuffled model loadings and the shuffled model loadings except for exposure at ages 9, 12, and 13 years (Wilcoxon tests, $p_{FDR} < .05$) (Table 2). All white matter tract loadings except for the right anterior thalamic radiation tract differed significantly between the unshuffled models and the shuffled models (Wilcoxon tests, $p_{FDR} < .05$) (Table 3). The top median loadings for the adversity variate were adversity experienced at ages 4 and 5 years followed by adversity experienced during ages 8, 3, and 6 years, respectively. All adversity variables loaded negatively. For the white matter variate, connectivity of the bilateral parietal occipital-pontine tracts, corticospinal tracts, superior thalamic radiation tracts, frontopontine tracts, and thalamo-premotor tracts loaded negatively. The left striato-fronto-orbital tract and corpus callosum rostrum loaded positively (Figure 3B).

Table 3. Loading Significance for Variables on the White Matter Variate of Mode 1 Across Models

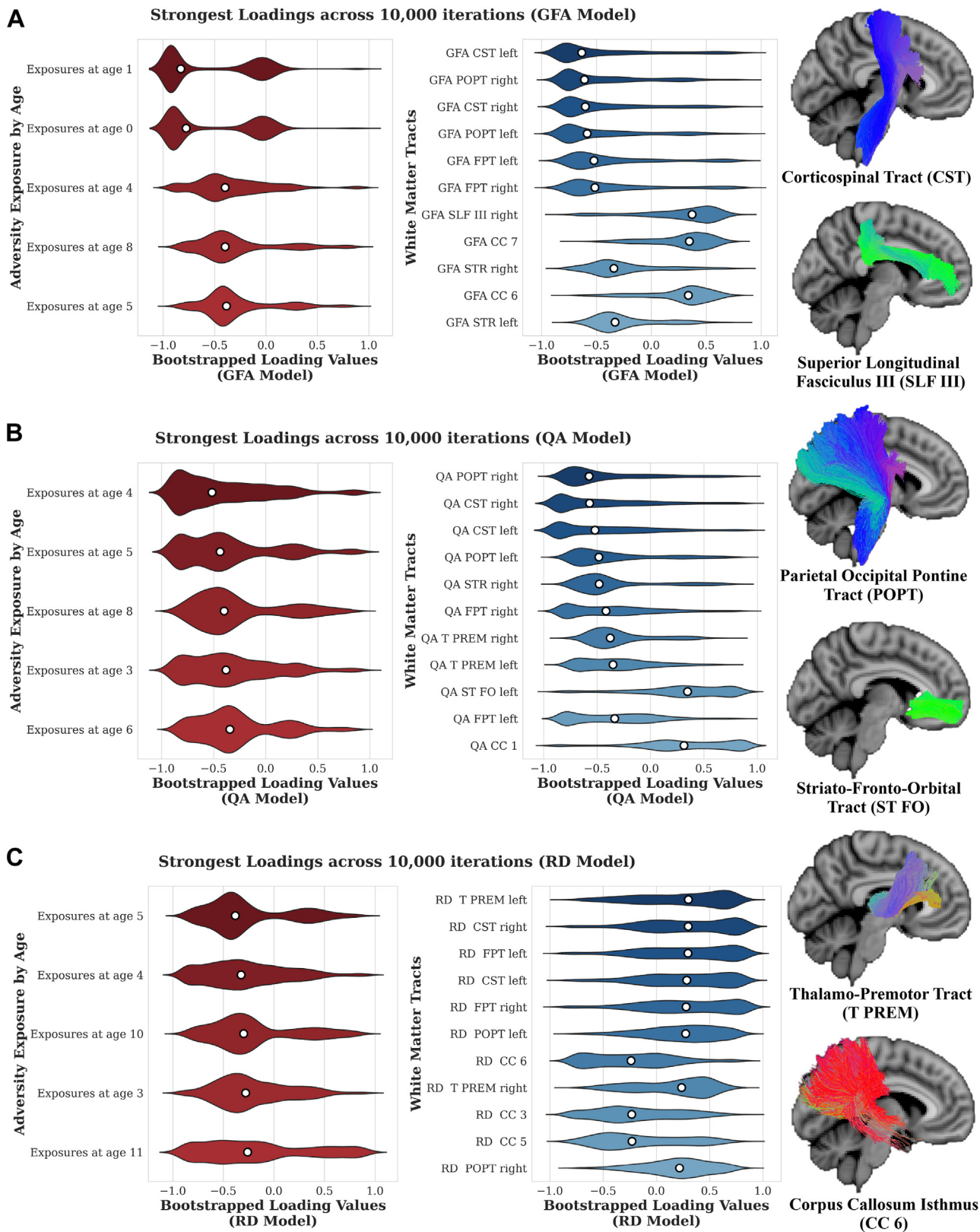
Variable	GFA Model		QA Model		RD Model	
	Wilcoxon Stat	p_{FDR}	Wilcoxon Stat	p_{FDR}	Wilcoxon Stat	p_{FDR}
AF Left	21,776,429	<.001	15,861,798	<.001	20,510,657	<.001
AF Right	14,363,325	<.001	22,459,308	<.001	24,498,424	.085
ATR Left	19,328,383	<.001	24,274,599	.012	15,842,749	<.001
ATR Right	17,036,998	<.001	24,770,880	.422	18,383,990	<.001
CC 1	11,897,415	<.001	11,478,426	<.001	20,478,464	<.001
CC 2	14,592,199	<.001	12,141,753	<.001	16,150,036	<.001
CC 3	14,088,000	<.001	18,086,639	<.001	16,096,523	<.001
CC 4	17,503,452	<.001	19,910,855	<.001	16,277,551	<.001
CC 5	19,693,682	<.001	23,487,830	<.001	17,973,792	<.001
CC 6	10,585,271	<.001	18,596,323	<.001	13,756,568	<.001
CC 7	9,207,805	<.001	14,508,115	<.001	19,902,098	<.001
CG Left	11,789,155	<.001	15,054,683	<.001	17,185,789	<.001
CG Right	12,828,612	<.001	18,965,772	<.001	14,115,177	<.001
CST Left	8,896,200	<.001	9,824,727	<.001	13,730,460	<.001
CST Right	8,446,158	<.001	8,786,120	<.001	13,054,342	<.001
FPT Left	10,738,831	<.001	11,910,354	<.001	14,177,189	<.001
FPT Right	11,129,139	<.001	10,815,098	<.001	14,157,857	<.001
IFO Left	12,932,951	<.001	15,607,634	<.001	24,173,215	.004
IFO Right	14,597,577	<.001	20,057,007	<.001	21,884,590	<.001
ILF Left	17,633,920	<.001	18,703,478	<.001	17,286,273	<.001
ILF Right	22,942,130	<.001	22,868,923	<.001	19,200,973	<.001
OR Left	18,295,807	<.001	19,557,512	<.001	21,434,711	<.001
OR Right	24,681,989	.267	22,598,513	<.001	23,227,519	<.001
POPT Left	8,008,802	<.001	10,376,115	<.001	12,822,688	<.001
POPT Right	7,315,601	<.001	8,972,140	<.001	13,973,584	<.001
SLF I Left	20,363,143	<.001	21,037,240	<.001	22,886,716	<.001
SLF I Right	22,115,273	<.001	17,695,373	<.001	21,177,870	<.001
SLF II Left	14,430,937	<.001	23,893,219	<.001	24,773,264	.427
SLF II Right	19,117,725	<.001	22,694,949	<.001	22,435,458	<.001
SLF III Left	10,809,319	<.001	12,810,510	<.001	15,921,669	<.001
SLF III Right	11,308,796	<.001	12,897,982	<.001	15,637,609	<.001
ST FO Left	18,719,173	<.001	12,148,092	<.001	21,932,082	<.001
ST FO Right	18,329,142	<.001	12,627,575	<.001	23,730,382	<.001
ST PREM Left	20,780,394	<.001	17,504,330	<.001	23,849,658	<.001
ST PREM Right	21,971,378	<.001	18,429,987	<.001	23,729,571	<.001
STR Left	11,586,699	<.001	12,337,193	<.001	17,890,569	<.001
STR Right	12,464,063	<.001	9,816,841	<.001	18,624,828	<.001
T PAR Left	12,287,328	<.001	17,956,494	<.001	18,037,106	<.001
T PAR Right	13,355,543	<.001	13,601,298	<.001	20,824,616	<.001
T PREM Left	11,579,977	<.001	10,963,186	<.001	15,204,527	<.001
T PREM Right	13,014,414	<.001	10,699,779	<.001	17,187,610	<.001
UF Left	13,346,019	<.001	13,237,168	<.001	24,571,801	.139
UF Right	13,786,856	<.001	13,774,513	<.001	24,198,066	.006

AF, arcuate fasciculus; ATR, anterior thalamic radiation; CC, corpus callosum; CC 1, CC rostrum; CC 2, CC genu; CC 3, CC rostral body (premotor); CC 4, CC anterior midbody (primary motor); CC 5, CC posterior midbody (primary somatosensory); CC 6, CC isthmus; CC 7, CC splenium; CG, cingulum cingulate; CST, corticospinal tract; FDR, false discovery rate; FPT, frontopontine tract; IFO, inferior fronto-occipital fasciculus; OR, optic radiation; POPT, parietal occipital-pontine tract; SLF, superior longitudinal fasciculus; ST FO, striato-fronto-orbital tract; STR, superior thalamic radiation; T PAR, thalamo-parietal tract; T PREM, thalamo-premotor tract; UF, uncinate fasciculus.

RD Model. For the RD model, all adversity exposure variables differed significantly between the unshuffled model loadings and the shuffled model loadings except for exposure at ages 6, 7, 8, and 15 years (Wilcoxon tests, $p_{FDR} < .05$)

(Table 2). All white matter tract loadings except for the left superior longitudinal fasciculus II tract, left uncinate fasciculus, and right arcuate fasciculus differed significantly from the shuffled model (Wilcoxon tests, $p_{FDR} < .05$) (Table 3). The top

Adversity Timing and White Matter Tract Connectivity



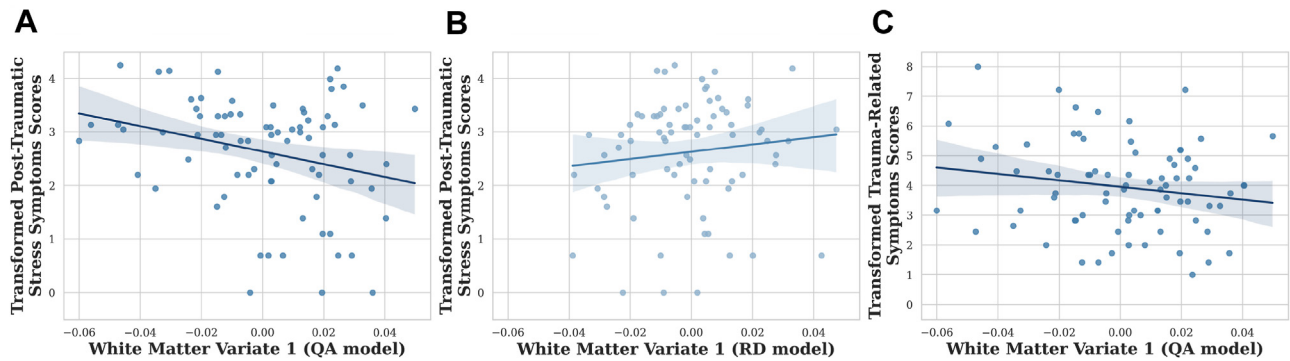


Figure 4. Associations between Reaction Index posttraumatic stress symptoms and (A) transformed values of the white matter variate from mode 1 of the quantitative anisotropy (QA) model averaged across 10,000 iterations of resampling, (B) transformed values of the white matter variate from mode 1 of the radial diffusivity (RD) model averaged across 10,000 iterations of resampling; (C) association between transformed values of the white matter variate from mode 1 of the QA model averaged across 10,000 iterations of resampling and transformed Trauma Symptom Checklist-40 trauma-related symptoms.

median loadings for the adversity variate were adversity experienced during ages 5 and 4 years, followed by adversity experienced during ages 10, 3, and 11 years, respectively. All adversity variables loaded negatively. For the white matter variate, bilateral thalamo-premotor tracts, corticospinal tracts, frontopontine tracts, parietal occipito-pontine tracts, and the right thalamo-premotor tract loaded positively, while the corpus callosum isthmus, rostral body, and posterior midbody loaded negatively (Figure 3C).

Associations with Mental Health Symptoms. Next, we tested whether the adversity and white matter variates from the 3 models were associated with symptoms among a subset of participants with data for posttraumatic stress symptoms (55), trauma-related symptoms (56), and total mental health symptoms (57). For each symptom measure, 2 OLS models were used to test whether 1) adversity variates and 2) white matter variates from the GFA, QA, and RD sCCA models were associated with symptoms. There was an association between RI posttraumatic stress symptoms and the QA model white matter variate ($t_{72} = -2.745$; $\beta = -0.324$; 95% CI, -0.559 to -0.089 ; $p = .008$) (Figure 4A) and a trend-level association with the RD model white matter variate ($t_{72} = 1.821$; $\beta = 0.226$; 95% CI, -0.021 to 0.473 ; $p = .073$) (Figure 4B). There was also a trend-level association between TSC-40 trauma-related symptoms and the QA model white matter variate ($t_{72} = -1.757$; $\beta = -0.292$; 95% CI, -0.624 to 0.039 ; $p = .083$) (Figure 4C). Finally, there were no significant associations between ASR total symptoms T scores and white matter variates (all p s $> .10$). There were also no associations between symptoms and the adversity variates across all 3 models (all p s $> .10$). The association between RI posttraumatic stress symptoms and the QA model white matter variate survived FDR correction ($p_{FDR} = .021$).

DISCUSSION

Adversity experienced during development can have profound effects on the brain and mental health; however, there is substantial heterogeneity in outcomes. In the current study, we leveraged a data-driven approach to investigate covariation between the developmental timing of adversity and white matter tract connectivity in adulthood. We observed a systematic pattern of covariation such that greater adversity exposure during preschool age and middle childhood was linked with higher connectivity of white matter tracts that subserve sensorimotor functions (e.g., corticospinal tract, corticopontine tracts) but lower connectivity of white matter tracts that subserve higher-order cortico-cortical communication (e.g., corpus callosum, superior longitudinal fasciculus). Across all 3 models (GFA, QA, RD), adversity exposure during ages 4 and 5 was linked to differential patterns of tract connectivity. For GFA and QA, adversity exposure at ages 4 and 5 was linked with lower connectivity of cortico-cortical tracts and higher connectivity of sensorimotor tracts. For RD, exposure at ages 4 and 5 was linked to higher RD (suggesting lower myelin content) in cortico-cortical tracts and lower RD (suggesting higher myelin content) in sensorimotor tracts. Because reduced myelination represents one cellular-level mechanism that may contribute to reduced tract connectivity indexed by GFA and QA, these results suggest a consistent adversity-linked pattern of increased connectivity in sensorimotor tracts and decreased connectivity in cortico-cortical tracts, possibly driven in part by differences in myelination. Furthermore, the white matter variate from the QA model was associated with posttraumatic stress symptoms, suggesting that patterns of decreased connectivity in cortico-cortical tracts and increased connectivity in sensorimotor tracts throughout the brain may underlie stress-related symptomatology.

Figure 3. Top loadings for adversity (left) and tract connectivity (right). The median loading value for each variable (white circle) is plotted on top of the distribution of bootstrapped loading values for that variable. The top 25% of tracts are displayed. (A) Loadings from the generalized fractional anisotropy (GFA) model. (B) Loadings from the quantitative anisotropy (QA) model. (C) Loadings from the radial diffusivity (RD) model. Segmented tract images from a representative participant are plotted on the far right. Additional loadings are displayed in Figure S7. CC, corpus callosum; CC 1, CC rostrum; CC 2, CC genu; CC 3, CC rostral body (premotor); CC 4, CC anterior midbody (primary motor); CC 5, CC posterior midbody (primary somatosensory); CC 7, CC splenium; CG, cingulum cingulate; FPT, frontopontine tract; STR, superior thalamic radiation.

Adversity Timing and White Matter Tract Connectivity

The finding that sensorimotor and cortico-cortical tracts showed inverse associations with exposure to adversity during preschool age and middle childhood suggests that adversity-associated, experience-dependent remodeling of structural connectivity may intersect with ongoing cortical neuro-development unfolding along the sensorimotor-association axis (10,12). Evidence from the RD model suggesting higher myelin content along sensorimotor tracts and lower myelin content along cortico-cortical tracts in association with preschool-age and preadolescent adversity implicates myelination as a possible cellular-level plasticity regulator underlying this pattern. Myelination has been shown to occur preferentially along active axonal pathways (37) and is further stimulated by experiencing acute stress during development (38), while attenuated signaling reduces axonal myelination (37). These results suggest the possibility that adversity during ages 4 to 5 in particular may activate experience-dependent myelination processes that prioritize structural connectivity that supports functions such as sensory perception and relay, while simultaneously deprioritizing structural connectivity that supports higher-order functions, such as complex cognitive and emotion processing, among cortical association regions. Although potentially adaptive during development (40), these changes may place individuals at greater risk for cognitive and emotional problems in the longer term (32,47).

The inverse pattern of associations with adversity that we observed across sensorimotor and cortico-cortical tracts, as represented in the QA variate, was significantly associated with posttraumatic stress symptoms. Building on well-documented associations between lower white matter connectivity in cortico-cortical tracts and greater mental health problems (47,50,52,53,78), these findings suggest the possibility that concomitant higher connectivity in tracts involved in sensorimotor processing may relate to other sequelae of adversity exposure, such as heightened sensory responsivity (79). Notably, none of the adversity variates from the GFA, QA, or RD models were associated with posttraumatic stress symptoms, suggesting that individual variation in adversity-linked whole-brain patterns of tract connectivity may mediate associations with later mental health. Interestingly, the association between white matter tract connectivity and mental health was specific to symptomatology linked to focal adverse events and not to more general trauma-related symptomatology, highlighting the importance of isolating variance in psychopathology related to particularly influential adverse events. Furthermore, the tract measures that comprised the top loadings of the QA variate were not individually associated with posttraumatic stress symptoms, suggesting that adversity-linked connectivity changes throughout the brain may be more relevant to mental health than localized alterations in specific tracts.

While adversity during preschool age and middle childhood emerged as top loadings across all 3 models, there was important variation by metric. Top loadings for the QA model most consistently represented adversity exposure during preschool age and middle childhood (ages 3–8). Because the QA white matter variate was associated with posttraumatic stress symptoms, these findings suggest that preschool age and middle childhood (in contrast to our initial hypothesis of early childhood) may represent a sensitive window during which

adversity may more readily get under the skin to shape white matter connectivity in a way that increases risk for later mental health problems. This finding also suggests that the increased specificity of QA in indexing directional fiber populations may yield metrics that better reflect circuit-specific changes, which in turn relate more closely to mental health.

Within the GFA model, adversity during early childhood (ages 0 and 1) comprised the first and second loadings. While these loadings suggest a large effect size, relatively sparse reports of adversity at these ages constrain our ability to draw inferences about this particular developmental stage. Furthermore, the GFA white matter variate was not associated with symptoms, suggesting that adversity during preschool age and middle childhood may be more strongly linked with changes in white matter structure that are clinically relevant during young adulthood. In the RD model, adversity during ages 9 to 10 comprised the third and fifth loadings, suggesting that adversity-associated changes in myelination patterns may be most prominent during preschool age and preadolescence. These results align with findings from rodent models that showed that adversity exposure during the juvenile period resulted in changes to prefrontal cortical myelination that lasted into adulthood (80).

While the current study contributes to the field's understanding of how the developmental timing of adversity may differentially shape white matter tracts and psychiatric risk, several limitations should be addressed in future research. First, this laboratory-based study comprised participants who completed time-intensive clinical interviews, which resulted in rich information on adversity exposure during development and mental health symptoms (54). This time-intensive phenotyping is critical to advancing the science of adversity exposure and brain development, but it practically constrains sample size. Therefore, we aimed to robustly characterize our sample by using resampling and permutation testing procedures (81) and by applying a multivariate approach (69). Recent work suggests that multivariate approaches may be better suited to detecting effects in modestly sized samples than univariate approaches (82,83); nonetheless, it will be important to replicate findings in a larger, more demographically diverse sample with information on adversity exposure timing. Relatedly, despite having rich information on adversity exposure, sample size precluded us from further parsing these events by additional relevant dimensions of adversity (3–6). Future work could build on these findings by examining the intersection of additional dimensions with developmental timing to elucidate how specific dimensions of adversity may relate to neuro-development, risk, and resilience.

Additionally, these findings should be interpreted in the context of retrospective report of adversity exposure. Participants might not have been able to accurately recall or report all adverse events at each age, or the ages at which events occurred, especially events experienced during early childhood (84). Despite these limitations (85), retrospectively reported measures demonstrate stronger associations with mental health symptoms than more objective measures of adversity (86,87). Furthermore, agreement between retrospective report and prospective report is higher when studies use interviews (instead of questionnaires), as in the current study (88). This study sample comprised primarily high-functioning young

adults and excluded participants with several comorbid diagnoses, thereby potentially reflecting a relatively stress-resilient population. Thus, how the current findings may differ among individuals with severe psychopathology remains to be explored. Future prospective studies that use large-scale longitudinal cohorts that systematically assess children's adversity exposure at each age are needed to clarify when and how adversity confers risk for psychiatric disorders, as well as elucidate how adversity at distinct developmental stages shapes neurodevelopmental trajectories.

Finally, the white matter tract metrics used in our study (GFA, QA, RD) represent macroscopic proxies for the underlying cellular structure of white matter tracts. GFA and QA are thought to index multiple cellular properties, including fiber organization, orientation, and myelination. GFA and RD, which are computed at the voxel level, may also be influenced by crossing fibers. While RD is the diffusion tensor metric thought to be most sensitive to myelin content (44), it should be noted that RD is not a direct index of the myelination process itself or of neuroplasticity. Future studies that leverage myelin-specific imaging sequences (89) will be important to further elucidate the role of myelination in adversity-related changes to white matter tract organization. Finally, we covaried for participant age in the current study, but some white matter tracts continue developing into adulthood. Future studies that use larger samples will be valuable for characterizing whether participant age moderates associations between white matter tract connectivity and adversity. Similarly, because the development of white matter tract connectivity may differ by sex (90), future studies that examine how associations between adversity, white matter connectivity, and mental health may differ by sex could elucidate sex-specific impacts and vulnerability.

Conclusions

This study identified multivariate links between the developmental timing of adversity and white matter tract connectivity as well as subsequent associations between latent patterns of white matter tract connectivity and mental health. Converging across diffusion metrics, latent variates representing adversity exposure during preschool age and middle childhood (primarily ages 4, 5, and 8 years) were associated with higher white matter connectivity of sensorimotor tracts and lower white matter connectivity of cortico-cortical and corticolimbic tracts. Our results suggest that adversity during preschool age and middle childhood may differentially shape white matter tract development in a circuit-specific manner, resulting in higher connectivity among sensorimotor tracts and lower connectivity among cortico-cortical tracts during adulthood. Experience-dependent myelination may represent one cellular-level mechanism that contributes to this pattern. This differential pattern of tract connectivity was associated with posttraumatic stress symptoms, suggesting that the neural underpinnings of stress-related psychopathology may be broadly distributed in tracts across the brain rather than being localized to a single tract or region. Taken together, these findings illuminate how adversity exposure may intersect with neurodevelopmental timing to differentially shape global white matter tract development and risk for mental health problems. Ultimately, better characterizing the role of developmental timing in associations

between adversity and maturing neural circuitry and behavior could inform the development of timely, individually tailored interventions to optimally support youths exposed to adversity.

ACKNOWLEDGMENTS AND DISCLOSURES

This work was supported by the National Science Foundation (NSF) Graduate Research Fellowship Program award (Award No. NSF DGE-1752134 [to LMS]) and a Dissertation Funding Award from the Society for Research in Child Development (to LMS); Yale Child Study Center Postdoctoral grant (Grant No. T32MH18268 [to TJK]) and NARSAD Young Investigator Award from the Brain & Behavior Research Foundation (Award No. 28436 [to TJK]); NSF Graduate Research Fellowship Program award (Award No. NSF DGE-1752134 [to EMC]), American Psychological Foundation Elizabeth Munsterberg Koppitz Child Psychology Graduate Fellowship, The Society for Clinical Child and Adolescent Psychology (division 53 of the American Psychological Association) Donald Routh Dissertation Grant, a Dissertation Funding Award from the Society for Research in Child Development, a Dissertation Research Award from the American Psychological Association, an American Dissertation Fellowship from the American Association of University Women, and a Scholar Award granted by the International Chapter of the Philanthropic Educational Organization (PEO Foundation) (to EMC); NSF Graduate Research Fellowship Program award (Award No. NSF DGE-1752134 [to PO]); Janet and Sheldon (1959) Razin Fellowship (Massachusetts Institute of Technology) (to SJZ); NSF CAREER Award (Award No. BCS-2145372 [to DGG]), National Institutes of Health Director's Early Independence Award (Award No. DP5OD021370 [to DGG]), NARSAD Young Investigator Award from the Brain & Behavior Research Foundation, Jacobs Foundation Early Career Research Fellowship, and The Society for Clinical Child and Adolescent Psychology (division 53 of the American Psychological Association) Richard Dick Abidin Early Career Award and Grant (to DGG).

DGG, LMS, EMC, and PO contributed to study design. LMS and DGG conceptualized and designed the analyses for this project. LMS analyzed the data. TJK reviewed code and analyses. EMC, SM, JCP, PO, SK, JTH, SJZ, HRH, LMS, and CC contributed to data collection. LMS, GG, AYH, AT, EMC, SM, JCP, and HRH contributed to quality assessment and data validation. LMS drafted the manuscript, and TJK, EMC, PO, SK, SJZ, HRH, GG, AYH, AT, and DGG reviewed and edited the manuscript.

A previous version of this article was published as a preprint on bioRxiv: <https://doi.org/10.1101/2023.11.12.566271>.

Code used to run QSIPrep preprocessing and reconstruction and TractSeg tractography can be found at https://github.com/Yale-CANLab/DWI_Code. The dataset and code used in this manuscript can be found at https://github.com/Yale-CANLab/Sisk_DWI_Adversity_sCCA.

The authors report no biomedical financial interests or potential conflicts of interest.

ARTICLE INFORMATION

From the Department of Psychology, Yale University, New Haven, Connecticut (LMS, TJK, EMC, SM, PO, SK, JTH, CC, GG, AYH, AT, DGG); Department of Psychology, the City College of New York, New York, New York (JCP); Interdepartmental Neuroscience Program, Yale School of Medicine, New Haven, Connecticut (SK); Department of Brain and Cognitive Sciences, Massachusetts Institute of Technology, Cambridge, Massachusetts (SJZ); and Institute of Child Development, University of Minnesota, Minneapolis, Minnesota (HRH).

Address correspondence to Dylan G. Gee, Ph.D., at dylan.gee@yale.edu.

Received Oct 25, 2024; revised Jan 17, 2025; accepted Feb 10, 2025.

Supplementary material cited in this article is available online at <https://doi.org/10.1016/j.bpsc.2025.02.003>.

REFERENCES

- Giano Z, Wheeler DL, Hubach RD (2020): The frequencies and disparities of adverse childhood experiences in the U.S. *BMC Public Health* 20:1327.
- Green JG, McLaughlin KA, Berglund PA, Gruber MJ, Sampson NA, Zaslavsky AM, Kessler RC (2010): Childhood adversities and adult

Adversity Timing and White Matter Tract Connectivity

- psychiatric disorders in the national comorbidity survey replication I: associations with first onset of DSM-IV disorders. *Arch Gen Psychiatry* 67:113–123.
3. Cohodes EM, Kitt ER, Baskin-Sommers A, Gee DG (2021): Influences of early-life stress on frontolimbic circuitry: Harnessing a dimensional approach to elucidate the effects of heterogeneity in stress exposure. *Dev Psychobiol* 63:153–172.
 4. McLaughlin KA, Sheridan MA, Humphreys KL, Belsky J, Ellis BJ (2021): The value of dimensional models of early experience: Thinking clearly about concepts and categories. *Perspect Psychol Sci* 16:1463–1472.
 5. Ellis BJ, Sheridan MA, Belsky J, McLaughlin KA (2022): Why and how does early adversity influence development? Toward an integrated model of dimensions of environmental experience. *Dev Psychopathol* 34:447–471.
 6. Smith KE, Pollak SD (2021): Rethinking concepts and categories for understanding the neurodevelopmental effects of childhood adversity. *Perspect Psychol Sci* 16:67–93.
 7. Gee DG, Casey BJ (2015): The impact of developmental timing for stress and recovery. *Neurobiol Stress* 1:184–194.
 8. Tottenham N, Sheridan MA (2009): A review of adversity, the amygdala and the hippocampus: A consideration of developmental timing. *Front Hum Neurosci* 3:68.
 9. Margulies DS, Ghosh SS, Goulas A, Falkiewicz M, Huntenburg JM, Langs G, *et al.* (2016): Situating the default-mode network along a principal gradient of macroscale cortical organization. *Proc Natl Acad Sci U S A* 113:12574–12579.
 10. Sydnor VJ, Larsen B, Seidlitz J, Adebimpe A, Alexander-Bloch AF, Bassett DS, *et al.* (2023): Intrinsic activity development unfolds along a sensorimotor–association cortical axis in youth. *Nat Neurosci* 26:638–649.
 11. Casey BJ (2015): Beyond simple models of self-control to circuit-based accounts of adolescent behavior. *Annu Rev Psychol* 66:295–319.
 12. Gogtay N, Giedd JN, Lusk L, Hayashi KM, Greenstein D, Vaituzis AC, *et al.* (2004): Dynamic mapping of human cortical development during childhood through early adulthood. *Proc Natl Acad Sci U S A* 101:8174–8179.
 13. Amso D, Lynn A (2017): Distinctive mechanisms of adversity and socioeconomic inequality in child development: A review and recommendations for evidence-based policy. *Policy Insights Behav Brain Sci* 4:139–146.
 14. Andersen SL (2003): Trajectories of brain development: Point of vulnerability or window of opportunity? *Neurosci Biobehav Rev* 27:3–18.
 15. Fox SE, Levitt P, Nelson CA (2010): How the timing and quality of early experiences influence the development of brain architecture. *Child Dev* 81:28–40.
 16. Sisk LM, Gee DG (2022): Stress and adolescence: Vulnerability and opportunity during a sensitive window of development. *Curr Opin Psychol* 44:286–292.
 17. Thomason ME, Marusak HA (2017): Toward understanding the impact of trauma on the early developing human brain. *Neuroscience* 342:55–67.
 18. Greenough WT, Black JE, Wallace CS (1987): Experience and brain development. *Child Dev* 58:539–559.
 19. Wiesel TN, Hubel DH (1963): Single-cell responses in striate cortex of kittens deprived of vision in one eye. *J Neurophysiol* 26:1003–1017.
 20. Sisk LM, Gee DG (2024): Developmental neuroplasticity and adversity-related risk for psychopathology. *Neuropsychopharmacology* 50:316–317.
 21. Gabard-Durnam L, McLaughlin KA (2020): Sensitive periods in human development: Charting a course for the future. *Curr Opin Behav Sci* 36:120–128.
 22. Frankenhuis WE, Walasek N (2020): Modeling the evolution of sensitive periods. *Dev Cogn Neurosci* 41:100715.
 23. Hardi FA, Goetschius LG, Peckins MK, Brooks-Gunn J, McLanahan SS, McLoyd V, *et al.* (2022): Differential developmental associations of material hardship exposure and adolescent amygdala-prefrontal cortex white matter connectivity. *J Cogn Neurosci* 34:1866–1891.
 24. Malter Cohen M, Jing D, Yang RR, Tottenham N, Lee FS, Casey BJ (2013): Early-life stress has persistent effects on amygdala function and development in mice and humans. *Proc Natl Acad Sci U S A* 110:18274–18278.
 25. Pechtel P, Lyons-Ruth K, Anderson CM, Teicher MH (2014): Sensitive periods of amygdala development: The role of maltreatment in pre-adolescence. *Neuroimage* 97:236–244.
 26. Humphreys KL, King LS, Sacchet MD, Camacho MC, Colich NL, Ordaz SJ, *et al.* (2019): Evidence for a sensitive period in the effects of early life stress on hippocampal volume. *Dev Sci* 22:e12775.
 27. McEwen BS, Nasca C, Gray JD (2016): Stress Effects on Neuronal Structure: Hippocampus, amygdala, and Prefrontal Cortex. *Neuropsychopharmacology* 41:3–23.
 28. Teicher MH, Samson JA, Anderson CM, Ohashi K (2016): The effects of childhood maltreatment on brain structure, function and connectivity. *Nat Rev Neurosci* 17:652–666.
 29. Andersen SL, Tomada A, Vincow ES, Valente E, Polcari A, Teicher MH (2008): Preliminary evidence for sensitive periods in the effect of childhood sexual abuse on regional brain development. *J Neuropsychiatry Clin Neurosci* 20:292–301.
 30. Hart H, Rubia K (2012): Neuroimaging of child abuse: A critical review. *Front Hum Neurosci* 6:52–52.
 31. Bick J, Zhu T, Stamoulis C, Fox NA, Zeanah C, Nelson CA (2015): Effect of early institutionalization and foster care on long-term white matter development: A randomized clinical trial. *JAMA Pediatr* 169:211–219.
 32. Hanson JL, Adluru N, Chung MK, Alexander AL, Davidson RJ, Pollak SD (2013): Early neglect is associated with alterations in white matter integrity and cognitive functioning. *Child Dev* 84:1566–1578.
 33. Howell BR, Ahn M, Shi Y, Godfrey JR, Hu X, Zhu H, *et al.* (2019): Disentangling the effects of early caregiving experience and heritable factors on brain white matter development in rhesus monkeys. *Neuroimage* 197:625–642.
 34. Reh RK, Dias BG, Nelson CA, Kaufer D, Werker JF, Kolb B, *et al.* (2020): Critical period regulation across multiple timescales. *Proc Natl Acad Sci U S A* 117:23242–23251.
 35. Hensch TK (2005): Critical period plasticity in local cortical circuits. *Nat Rev Neurosci* 6:877–888.
 36. Forbes TA, Gallo V (2017): All wrapped up: Environmental effects on myelination. *Trends Neurosci* 40:572–587.
 37. Mitew S, Gobius I, Fenlon LR, McDougall SJ, Hawkes D, Xing YL, *et al.* (2018): Pharmacogenetic stimulation of neuronal activity increases myelination in an axon-specific manner. *Nat Commun* 9:306.
 38. Osso LA, Rankin KA, Chan JR (2021): Experience-dependent myelination following stress is mediated by the neuropeptide dynorphin. *Neuron* 109:3619–3632.e5.
 39. Ho TC, King LS (2021): Mechanisms of neuroplasticity linking early adversity to depression: Developmental considerations. *Transl Psychiatry* 11:517.
 40. Ellis BJ, Del Giudice M (2019): Developmental adaptation to stress: An evolutionary perspective. *Annu Rev Psychol* 70:111–139.
 41. Tuch DS (2004): Q-ball imaging. *Magn Reson Med* 52:1358–1372.
 42. Yeh F-C, Wedeen VJ, Tseng W-YI (2010): Generalized Q-sampling imaging. *IEEE Trans Med Imaging* 29:1626–1635.
 43. Alexander AL, Lee JE, Lazar M, Field AS (2007): Diffusion tensor imaging of the brain. *Neurotherapeutics* 4:316–329.
 44. Winkiewski PJ, Sabisz A, Naumczyk P, Jodzio K, Szurowska E, Szarmach A (2018): Understanding the physiopathology behind axial and radial diffusivity changes-what do we know? *Front Neurol* 9:92.
 45. Lim L, Howells H, Radua J, Rubia K (2020): Aberrant structural connectivity in childhood maltreatment: A meta-analysis. *Neurosci Biobehav Rev* 116:406–414.
 46. Larsen B, Cui Z, Adebimpe A, Pines A, Alexander-Bloch A, Bertolero M, *et al.* (2022): A developmental reduction of the excitation:inhibition ratio in association cortex during adolescence. *Sci Adv* 8:eabj8750.
 47. Bick J, Fox N, Zeanah C, Nelson CA (2017): Early deprivation, atypical brain development, and internalizing symptoms in late childhood. *Neuroscience* 342:140–153.
 48. Shonkoff JP, Garner AS, Committee on Psychosocial Aspects of Child and Family Health, Committee on Early Childhood, Adoption, and Dependent Care, Section on Developmental and Behavioral Pediatrics (2012): The lifelong effects of early childhood adversity and toxic stress. *Pediatrics* 129:e232–e246.

49. De Bellis MD, Keshavan MS, Clark DB, Casey BJ, Giedd JN, Boring AM, *et al.* (1999): A.E. Bennett Research Award. Developmental traumatology. Part II: brain development. *Biol Psychiatry* 45:1271–1284.
50. O'Doherty DCM, Ryder W, Paquola C, Tickell A, Chan C, Hermens DF, *et al.* (2018): White matter integrity alterations in post-traumatic stress disorder. *Hum Brain Mapp* 39:1327–1338.
51. Jenkins LM, Barba A, Campbell M, Lamar M, Shankman SA, Leow AD, *et al.* (2016): Shared white matter alterations across emotional disorders: A voxel-based meta-analysis of fractional anisotropy. *Neuroimage Clin* 12:1022–1034.
52. Xu EP, Nguyen L, Leibenluft E, Stange JP, Linke JO (2023): A meta-analysis on the uncinate fasciculus in depression. *Psychol Med* 53:2721–2731.
53. Hanson JL, Knodt AR, Brigid BD, Hariri AR (2015): Lower structural integrity of the uncinate fasciculus is associated with a history of child maltreatment and future psychological vulnerability to stress. *Dev Psychopathol* 27:1611–1619.
54. Cohodes EM, McCauley S, Pierre JC, Hodges HR, Haberman JT, Santiuste I, *et al.* (2023): Development and validation of the Dimensional Inventory of Stress and Trauma Across the Lifespan (DISTAL): A novel assessment tool to facilitate the dimensional study of psychobiological sequelae of exposure to adversity. *Dev Psychobiol* 65:e22372.
55. Steinberg AM, Brymer MJ, Decker KB, Pynoos RS (2004): The University of California at Los Angeles Post-traumatic Stress Disorder Reaction Index. Available at: <https://link.springer.com/content/pdf/10.1007%2Fs11920-004-0048-2.pdf>. Accessed February 20, 2020.
56. Elliott DM, Briere J (1992): Sexual abuse trauma among professional women: Validating the Trauma Symptom Checklist-40 (TSC-40). *Child Abuse Negl* 16:391–398.
57. Rescorla LA, Achenbach TM (2004): The Achenbach System of Empirically Based Assessment (ASEBA) for ages 18 to 90 years. In: *The Use of Psychological Testing for Treatment Planning and Outcomes Assessment: Instruments for Adults*, 3rd ed, vol. 3. Mahwah, NJ: Lawrence Erlbaum Associates Publishers, 115–152.
58. Fischl B (2012): FreeSurfer. *Neuroimage* 62:774–781.
59. Cieslak M, Cook PA, He X, Yeh F-C, Dholander T, Adebimpe A, *et al.* (2021): QSIprep: An integrative platform for preprocessing and reconstructing diffusion MRI data. *Nat Methods* 18:775–778.
60. Avants BB, Tustison NJ, Song G, Cook PA, Klein A, Gee JC (2011): A reproducible evaluation of ANTs similarity metric performance in brain image registration. *Neuroimage* 54:2033–2044.
61. Zhang Y, Brady M, Smith S (2001): Segmentation of brain MR images through a hidden Markov random field model and the expectation-maximization algorithm. *IEEE Trans Med Imaging* 20:45–57.
62. Tournier J-D, Smith R, Raffelt D, Tabbara R, Dholander T, Pietsch M, *et al.* (2019): MRtrix3: A fast, flexible and open software framework for medical image processing and visualisation. *Neuroimage* 202:116137.
63. Tustison NJ, Avants BB, Cook PA, Zheng Y, Egan A, Yushkevich PA, Gee JC (2010): N4ITK: Improved N3 bias correction. *IEEE Trans Med Imaging* 29:1310–1320.
64. Andersson JLR, Sotiropoulos SN (2016): An integrated approach to correction for off-resonance effects and subject movement in diffusion MR imaging. *Neuroimage* 125:1063–1078.
65. Wasserthal J, Neher P, Maier-Hein KH (2018): TractSeg – Fast and accurate white matter tract segmentation. *Neuroimage* 183:239–253.
66. van Rossum G (1995): Python tutorial. Available at: <https://ir.cwi.nl/pub/5007>. Accessed November 11, 2023.
67. R Core Team (2019): R: A Language and Environment for Statistical Computing, version 3.6.1. Vienna, Austria: R Foundation for Statistical Computing. Available at: <https://www.R-project.org/>. Accessed May 15, 2020.
68. Chapman J, Wang H-T (2021): CCA-Zoo: A collection of Regularized, Deep Learning based, Kernel, and Probabilistic CCA methods in a scikit-learn style framework. *J Open Source Softw* 6:3823.
69. Witten DM, Tibshirani R, Hastie T (2009): A penalized matrix decomposition, with applications to sparse principal components and canonical correlation analysis. *Biostatistics* 10:515–534.
70. Wang H-T, Smallwood J, Mourao-Miranda J, Xia CH, Satterthwaite TD, Bassett DS, Bzdok D (2020): Finding the needle in a high-dimensional haystack: Canonical correlation analysis for neuroscientists. *Neuroimage* 216:116745.
71. Xia CH, Ma Z, Ciric R, Gu S, Betzel RF, Kaczkurkin AN, *et al.* (2018): Linked dimensions of psychopathology and connectivity in functional brain networks. *Nat Commun* 9:3003.
72. Benjamini Y, Hochberg Y (1995): Controlling the false discovery rate: A practical and powerful approach to multiple testing. *J R Stat Soc B* 57:289–300.
73. Rakesh D, Whittle S (2021): Socioeconomic status and the developing brain - A systematic review of neuroimaging findings in youth. *Neurosci Biobehav Rev* 130:379–407.
74. Tooley UA, Mackey AP, Ciric R, Ruparel K, Moore TM, Gur RC, *et al.* (2020): Associations between neighborhood SES and functional brain network development. *Cereb Cortex* 30:1–19.
75. Maholmes V, King RB (2012): *The Oxford Handbook of Poverty and Child Development*. Oxford, United Kingdom: Oxford University Press.
76. Winkler AM, Renaud O, Smith SM, Nichols TE (2020): Permutation inference for canonical correlation analysis. *Neuroimage* 220:117065.
77. Wilcoxon F (1945): Individual comparisons by ranking methods. *Biom Bull* 1:80–83.
78. Jackowski AP, Douglas-Palumberi H, Jackowski M, Win L, Schultz RT, Staib LW, *et al.* (2008): Corpus callosum in maltreated children with posttraumatic stress disorder: A diffusion tensor imaging study. *Psychiatry Res* 162:256–261.
79. Leal ASM, Alba LA, Cummings KK, Jung J, Waizman YH, Moreira JFG, *et al.* (2023): Sensory processing challenges as a novel link between early caregiving experiences and mental health. *Dev Psychopathol* 35:1968–1981.
80. Makinodan M, Rosen KM, Ito S, Corfas G (2012): A critical period for social experience-dependent oligodendrocyte maturation and myelination. *Science* 337:1357–1360.
81. Holt CA, Sullivan SP (2023): Permutation tests for experimental data. *Exp Econ* 26:775–812.
82. Marek S, Tervo-Clemmens B, Calabro FJ, Montez DF, Kay BP, Hatoum AS, *et al.* (2022): Reproducible brain-wide association studies require thousands of individuals. *Nature* 603:654–660.
83. Spisak T, Bingel U, Wager TD (2023): Multivariate BWAS can be replicable with moderate sample sizes. *Nature* 615:E4–E7.
84. Williams LM (1994): Recall of childhood trauma: A prospective study of women's memories of child sexual abuse. *J Consult Clin Psychol* 62:1167–1176.
85. Brewin CR, Andrews B, Gotlib IH (1993): Psychopathology and early experience: A reappraisal of retrospective reports. *Psychol Bull* 113:82–98.
86. Baldwin JR, Coleman O, Francis ER, Danese A (2024): Prospective and retrospective measures of child maltreatment and their association with psychopathology: A systematic review and meta-analysis. *JAMA Psychiatry* 81:769–781.
87. Francis ER, Tsaligopoulou A, Stock SE, Pingault J-B, Baldwin JR (2023): Subjective and objective experiences of childhood adversity: A meta-analysis of their agreement and relationships with psychopathology. *J Child Psychol Psychiatry* 64:1185–1199.
88. Baldwin JR, Reuben A, Newbury JB, Danese A (2019): Agreement between prospective and retrospective measures of childhood maltreatment: A systematic review and meta-analysis. *JAMA Psychiatry* 76:584–593.
89. Laule C, Moore GRW (2018): Myelin water imaging to detect demyelination and remyelination and its validation in pathology. *Brain Pathol* 28:750–764.
90. Lawrence KE, Abaryan Z, Laltoo E, Hernandez LM, Gandal MJ, McCracken JT, Thompson PM (2023): White matter microstructure shows sex differences in late childhood: Evidence from 6797 children. *Hum Brain Mapp* 44:535–548.